crystals

MDPI

Review

Characterising Supramolecular Architectures in Crystals Featuring I···Br Halogen Bonding: Persistence of X···X′ Secondary-Bonding in Their Congeners

Edward R. T. Tiekink

Research Centre for Crystalline Materials, School of Medical and Life Sciences, Sunway University, Bandar Sunway 47500, Malaysia; edwardt@sunway.edu.my; Tel.: +60-3-7491-7181

Abstract: The Cambridge Structural Database was surveyed for crystals featuring I···Br secondary-bonding in their supramolecular assemblies occurring independently of other obvious supramolecular synthons and devoid of other halogen bonding interactions. In all, 41 crystals satisfied these criteria, with nine examples of zero-dimensional aggregation (uniformly two-molecule aggregates) and 30 one-dimensional chains of varying topology (linear, zigzag and helical). There is one example each of two- and three-dimensional patterns. Type-I, type-II and intermediate bonding situations are apparent; for type-II bonding, the ratio of iodide:bromide functioning as the electrophile is 2:1. Most molecules participated, on average, in one I···Br contact, although smaller numbers of half (zero-dimensional) or two contacts (two- and three-dimensional) were observed. The propensity of the formation of related halogen bonding interactions in congeners of the 41 investigated crystals was also studied. Congeners were apparent for 11 crystals, with seven of these exhibiting isostructural relationships, in terms of space-group symmetry and unit-cell parameters. Isostructural relationships do not ensure the formation of analogous aggregation patterns, particularly and in accord with expectation, for the lighter halides. When formed, often distinct aggregation patterns are observed despite the isostructural relationships. Hetero-atomic halogen bonding offers surprises and opportunities in crystal engineering endeavours.

Keywords: secondary-bonding; halogen bonding; I···Br contacts; X···X′ contacts; supramolecular chemistry; σ–hole; coordination polymers; crystal structures

Citation: Tiekink, E.R.T. Characterising Supramolecular Architectures in Crystals Featuring I···Br Halogen Bonding: Persistence of X···X′ Secondary-Bonding in Their Congeners. *Crystals* **2021**, *11*, 433. https://doi.org/10.3390/cryst11040433

Academic Editors: Sergiy Rosokha and Atash V. Gurbanov

Received: 26 March 2021
Accepted: 13 April 2021
Published: 16 April 2021

1. Introduction

In supramolecular chemistry, halogen bonding refers to the phenomenon whereby a halide atom engages in an attractive interaction with an electron-rich site. X-ray crystallographic evidence for such an interaction dates back to a report in 1954 [1] where a supramolecular, one-dimensional chain was formed in the 1:1 multi-component crystal formed between Br_2 and dioxane, Figure 1. The magnitude of the Br···O separation is 2.72 Å, a value intermediate between the sum of the covalent radii (1.89 Å) and van der Waals radii (3.37 Å) for bromide and oxygen [2]; the Br–Br···O angle is almost linear at 178.3°. This mode of assessment for a non-covalent interaction based on distance criteria establishes the Br···O interaction under the aegis, "secondary-bonding interaction" [3], a concept built upon earlier reviews of molecules presenting similar non-covalent interactions [4–6]. In its simplest form, a "secondary-bonding interaction" may be defined as an intermolecular contact between a pair of atoms occurring beyond the sum of their covalent radii and below the sum of their van der Waals radii [3], and therefore is most conveniently identified in X-ray crystal structures. In this respect, this term covers interactions which are now classified as halogen bonding interactions; indeed, Alcock highlighted halogen bonding interactions in the review entitled "Secondary-bonding to nonmetallic elements" [3]. While the focus in the present commentary is upon X-ray crystallographic experiments, it

must be noted that experimental evidence for related secondary-bonding/halogen bonding interactions occurring between I_2 and NH_3 dates back over two centuries [7,8].

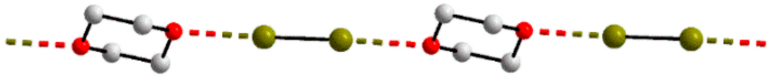

Figure 1. A view of a portion of the one-dimensional chain formed in the 1:1 multi-component crystal comprising Br_2 and dioxane. The molecule lies on a mirror plane as do the oxygen atoms of the dioxane molecule. Further, each component is disposed over a centre of inversion. The colour code in this and subsequent diagrams: bromide, dark green; oxygen, red; carbon, grey. Non-acidic hydrogen atoms are omitted for reasons of clarity. The halogen bond is represented by the dashed, multi-coloured bond coded in accordance with the participating atoms, in this case dark green and red.

While the interaction of two ostensibly electron-rich species might be perplexing, this is resolved in terms of the result of an anisotropic distribution of electron density around the halide atom. As introduced by Politzer et al. [9], there is an electron-deficient region at the extension of a, for example, C–X bond, where X is a halide with a build-up of electron density around the belt of the atom, which is perpendicular to the C–X bond in three dimensions. This distribution leads to a patch at the tip of X, termed a σ–hole, capable of behaving as an electrophile towards various nucleophiles, D, that typically but not exclusively include oxygen, nitrogen, sulphur or, relevant to the present study, another halide [9–11]. As most halides form a single covalent bond, C–X$\cdots$D halogen bonds are linear or close to linear, implying a high tendency towards directionality. This feature, coupled by the strength of these interactions, that is, akin to conventional hydrogen bonding interactions, gives rise to obvious parallels between halogen and hydrogen bonding [12–15]. Under comparable circumstances, the strength of a halogen bond follows the order I > Br > Cl >> F, reflecting the greater polarizability of iodide compared with the lighter halides. However, altering the nature of the carbon (or indeed other atom) bound to the halide through the moderation of electronic and/or steric effects allows for fine tuning of the strength and directionality of a putative halogen bonding interaction. This opens up a gamut of potential applications based on halogen bonding [16–18], not just for crystalline materials—for example, soft materials [19]—in the solution state [20–22] and in biologically relevant systems [23,24], and not exclusively for organic systems but those involving halide bound to metals [25–27]. Halogen bonding is now a mature discipline in supramolecular chemistry, including in crystal engineering endeavours [28,29].

Herein, in continuation of systematic surveys of non-covalent interactions operating in the crystals of main group element compounds [30–36] and more recently, halides participating in delocalised X$\cdots\pi$(arene) interactions [37], an analysis of crystal structures included in the Cambridge Structural Database (CSD) [38] for a relatively rare class of secondary-bonding interaction is undertaken, namely hetero-halide interactions involving iodide interacting with bromide. As indicated above, iodide is anticipated to form the strongest halogen bonding interactions, at least under comparable conditions, and it was thought to be of interest to ascertain the robustness of this precept in the presence of its most potent likely competitor, namely bromide, in crystals where both elements are present. In the first part of this analysis, the supramolecular architectures featuring I$\cdots$Br interactions operating independently of other supramolecular associations such as hydrogen bonding and other halogen bonding are described and categorised in terms of the dimension of the resulting aggregation pattern. Following this, congeners of the crystals categorised in the first part are identified in the CSD and an analysis undertaken for the presence of analogous X$\cdots$X′ interactions, where X and X′ are the same or different halides, in order to assess the pervasiveness of such contacts in crystals, as X and X′ are systematically varied.

2. Methods

The data discussed in this bibliographic review of the crystallographic literature were obtained after a systematic search of the Cambridge Structural Database (CSD, version 5.41 and three updates) [38] with the use of the integrative program ConQuest (version 2.0.4) [39]. The analysis entailed the search of all crystal structures featuring I···Br contacts less than the sum of the van der Waals radii of iodide (1.98 Å) and bromide (1.75 Å), that is, 3.83 Å; the chosen van der Waals radii are as in the CSD. Crystal structures that had disorders, had errors, contained ions, were polymeric and had transition metal or main group elements heavier than selenium were excluded. The search returned 63 structures which were filtered to removed duplicates and structures where the putative I···Br interaction was cooperating with hydrogen bonding or some other recognised supramolecular association. This resulted in 58 independent crystal structures. In order to enable a focus on the impact of I···Br interactions upon the molecular packing, the structures were then evaluated for additional halogen bonding interactions. Those crystals that featured extra X···X′ contacts linking the aggregates established by I···Br contacts were removed from the dataset. The full composition details for each of the 41 crystals satisfying the above criteria are given in Supplementary Materials Table S1, along with diagrams and a description of the aggregation pattern, as well as comments of additional intermolecular interactions whenever relevant. All crystallographic diagrams are original and were generated employing DIAMOND [40] using the data included in the Crystallographic Information File obtained from the CSD for each structure. The crystallographic analysis program PLATON [2] was employed routinely throughout the evaluation of the molecular packing in the studied crystals.

3. Supramolecular Aggregation Featuring I···Br Secondary-Bonding Interactions

Table 1 provides a summary of the crystals exhibiting I···Br secondary-bonding interactions described in this survey. In all, there were 41 examples of crystals exhibiting I···Br interactions [41–75] with key geometric parameters defining the I···Br interaction, namely the I···Br separation as well as C–I···Br and C–Br···I angles included in Table 1, along with a summary of the supramolecular assembly featuring the I···Br interaction(s), the CSD REFCODE and literature citation.

Table 1. Summary of geometric parameters (Å,°) and aggregation features for **1**–**41**.

Crystal	d(I···Br)	C–I···Br (θ_1)	C–Br···I (θ_2)	Motif	CSD REFCODE	Ref.
1	3.6830(11)	161.3(2)	102.6(2)	Two-molecule–one contact	OJACUY	[41]
2	3.7397(9)	172.38(19)	85.37(16)	Two-molecule–one contact	RECROI	[42]
3	3.813(3)	117.2(5)	161.2(5)	Two-molecule–one contact	DUPNIN	[43]
4	3.5640(3)	73.4(3)	159.70(4)	Centrosymmetric dimer	NEYSUG	[44]
5	3.6449(9)	160.07(13)	124.72(15)	Centrosymmetric dimer	LOBHOB	[45]
6	3.7068(13)	168.8(2)	102.8(3)	Centrosymmetric dimer	SIZTED	[46]
7	3.7556(4)	93.01(5)	155.75(6)	Centrosymmetric dimer	QOCSUZ	[47]
8	3.8122(5)	117.83(10)	166.26(12)	Centrosymmetric dimer	KAGQUH	[48]
9	3.6927(7)	156.68(11)	130.84(14)	Two-molecule–one contact	VIXWIL	[49]
10	3.5402(4)	169.74(9)	121.58(9)	1-D: linear	MUKKUY	[50]
11	3.540(2)	173.67(16)	91.44(19)	1-D: linear	MAMFIS	[51]
12	3.6421(9)	161.23(11)	160.90(13)	1-D: linear	SUWKUT	[52]

Table 1. *Cont.*

Crystal	d(I···Br)	C–I···Br (θ_1)	C–Br···I (θ_2)	Motif	CSD REFCODE	Ref.
13	3.6623(10)	155.87(8)	160.15(9)	1-D: linear	CIQMEV	[53]
14	3.7163(11)	84.5(3)	148.8(3)	1-D: linear	CORZER	[54]
15	3.7169(12)	149.09(17)	140.37(19)	1-D: linear	VIQQIC	[55]
16	3.7226(16)	166.3(3)	112.8(3)	1-D: linear	HIRHUM	[56]
17	3.7228(12)	158.5(2)	135.2(2)	1-D: linear	QAPQAC	[57]
18 [a]	3.6869(15)	162.8(2)	161.1(3)	1-D: linear	YIRTOJ	[58]
	3.7413(15)	159.8(3)	156.0(3)	1-D: linear		
19	3.7558(13)	84.5(3)	171.2(4)	1-D: linear	CABCAM	[59]
20	3.6271(4)	166.66(7)	97.45(10)	1-D: linear	MESMED	[60]
21	3.6011(6)	175.22(11)	103.29(13)	1-D: zigzag	YIZFUL	[61]
22	3.640(1)	168.25(17)	118.41(17)	1-D: zigzag	JIPTEK	[62]
23	3.6666(12)	175.7(2)	115.3(2)	1-D: zigzag	SELYOY	[63]
24	3.691(3)	151.5(4)	126.0(5)	1-D: zigzag	JINJUO	[64]
25 [b]	3.7380(17)	127.2(3)	151.3(4)	1-D: zigzag	MOZTED	[65]
	3.7905(14)	126.8(3)	158.3(4)			
26	3.8025(5)	127.28(11)	152.94(12)	1-D: zigzag	BULZIU	[66]
27	3.6889(8)	169.87(9)	138.90(11)	1-D: helical	BUNBAQ	[66]
28	3.6943(4)	170.95(7)	90.81(11)	1-D: helical	CIQLEU	[67]
29	3.7136(15)	78.41(9)	170.13(11)	1-D: helical	IMURAL	[68]
30	3.7281(18)	71.91(14)	161.19(15)	1-D: helical	INADIM	[68]
31	3.7330(7)	162.62(7)	81.66(7)	1-D: helical	IMUQOY	[68]
32	3.7592(4)	173.40(6)	104.68(8)	1-D: helical	FABWIR	[69]
33	3.7631(7)	87.09(15)	168.75(18)	1-D: helical	ZIMLIT	[70]
34	3.7724(9)	167.18(16)	76.25(18)	1-D: helical	WUJYUY	[71]
35	3.7966(13)	107.0(3)	160.7(3)	1-D: helical	IKUZAR	[72]
36	3.7973(9)	103.12(13)	159.62(14)	1-D: helical	GUMMEI	[73]
37	3.8053(7)	103.40(10)	159.58(11)	1-D: helical	GUMLUZ	[73]
38	3.8001(10)	165.44(11)	121.92(14)	1-D: helical	VEXDAG	[74]
39	3.8140(9)	169.03(7)	77.36(8)	1-D: helical	IMURUF	[68]
40 [c]	3.7436(5)	158.64(11)	87.49(12)	2-D; flat topology	VEGSOR	[75]
	3.7465(6)	80.73(11)	172.51(12)			
41	3.6944(7)	161.40(5)	83.20(5)	3-D	INADOS	[68]
	3.7405(5)	95.99(5)	155.52(5)			

[a] Two independent chains in the crystal; [b] Two independent molecules associated to form the chain; [c] Two independent contacts involving the same iodide atom.

The benchmark for determining the presence of a I···Br (and later in Section 4, X···X contacts in general) is a comparison of the separation between the two halide atoms to their respective sum of the van der Waals radii. While this does not imply that there is no interaction between a pair of halide atoms beyond the sum of the van der Waals radii [76–79], this criterion was applied to ensure some level of consistency in the analysis. The following description of the supramolecular assemblies is broken down into zero-dimensional aggregates (Section 3.1), followed by one-dimensional assemblies (Section

3.2) and then the relatively small number of two- and three-dimensional architectures (Section 3.3). Within each category, the aggregates are discussed in terms of increasing numbers of I···Br interactions featured within the assembly, single component crystals are described before multi-component crystals and the aggregates are listed in order of increasing values of the I···Br separations. Before embarking on the description of the supramolecular aggregation mediated by I···Br interactions, the geometric definitions of X···X′ halogen bonding need to be stated.

The widely adopted classification of halogen bonding interactions occurring between halides is illustrated in Figure 2 [80,81].

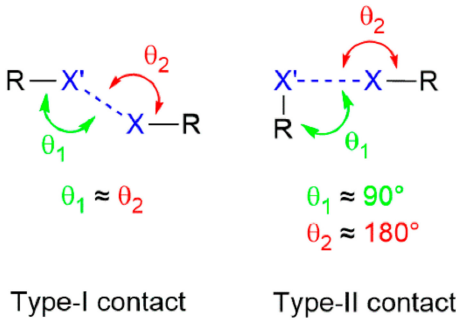

Figure 2. Schematic showing type-I and type-II interactions occurring between halides.

In a type-I contact, which often occurs around a centre of inversion, the θ_1 and θ_2 angles subtended at each halide are close to each other and at the extreme, each are 180°. Type-I contacts often occur at van der Waals separations and arise from global packing considerations. These may be found for all halides and can be weakly attractive or repulsive. Contrasting this symmetric arrangement is the distinctly bent configuration noted for type-II contacts. Type-II contacts relate to the nature of the interaction, that is, a σ–bonding interaction between an electrophile and a nucleophile. Such arrangements are more likely found for the heavier halides, bromide and iodide.

3.1. Zero-Dimensional Aggregates Featuring I···Br Interactions

The chemical diagrams for **1**–**9**, representing molecules presenting I···Br secondary-bonding interactions in their crystals leading to zero-dimensional aggregates, are shown in Figure 3. The first structural motif to be described is a two-molecule aggregate having a single I···Br interaction between them, as found in **1** [41], **2** [42] and **3** [43]. The interaction occurs between two molecules comprising the crystallographic asymmetric unit, implying one molecule is functioning as the donor and the other as the acceptor. In **1**, four independent molecules comprise the asymmetric unit but only two molecules participate in I···Br interactions. The other pair are also orientated to form a putative I···Br interaction but the separation is beyond the van der Waals limits (Table S1). In the aggregate formed in **2**, a weaker, supportive Br···Br contact is evident (Table S1). Two prototype aggregates found in the crystals of **1** and **3**, are illustrated in Figure 4a,b, respectively.

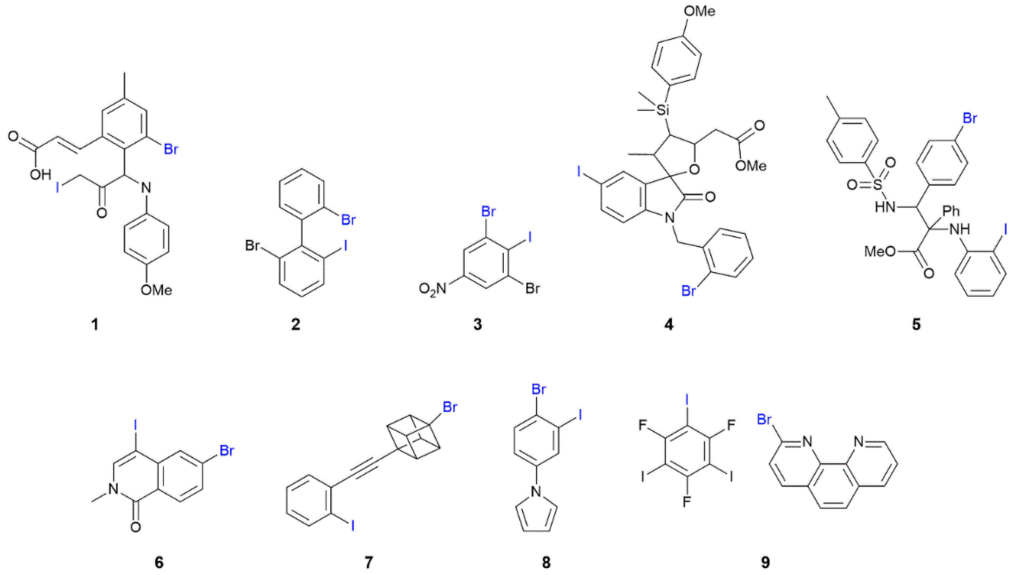

Figure 3. Chemical diagrams for molecules that form I···Br interactions in their crystals leading to zero-dimensional aggregation patterns (**1**–**9**). The atoms highlighted in blue are the atoms forming the I···Br interaction.

Referring to Table 1, based on the C–I···Br angle of 161.3(2)° in **1**, the anticipated I···Br halogen bond is formed consistent with the more polarisable iodide atom accepting electron density from the bromide atom, which is functioning as an electrophile. The C–Br···I angle of 102.6(2)°, indicative of a side-on approach, is consistent with this assignment as it indicates the bromide is functioning as the nucleophile. However, in **3**, the opposite trend is apparent with θ_1 = 117.2(5) and θ_2 = 161.2(5)°, where, based on these angle criteria, the bromide atom is functioning as the electrophile, Table 1. This interchange of roles is found repeatedly throughout the aggregates discussed in this survey.

The next structural motif also involves two molecules but these are connected over a centre of inversion via two I···Br contacts. This motif is adopted in the crystals of **4** [44], **5** [45], **6** [46], **7** [47] and **8** [48]. In each of **4** and **6**, two independent molecules comprise the asymmetric unit, but only one self-associates across an inversion centre; in **6**, the second independent molecule associates into a dimer via Br···Br halogen bonding contacts (Table S1). In **5** and **6**, Figure 4c, the iodide atom is functioning as the electrophile, while in **4**, **7**, Figure 4d, and **8**, the bromide adopts this role.

The sole co-crystal covered in this survey, namely **9** [49], comprises one molecule of each co-former and these are connected into a two-molecule aggregate via a single I···Br interaction, Figure 4e. It is noteworthy the C–I···Br and C–Br···I angles of 156.68(11) and 130.84(14)°, respectively, are relatively close together (see below).

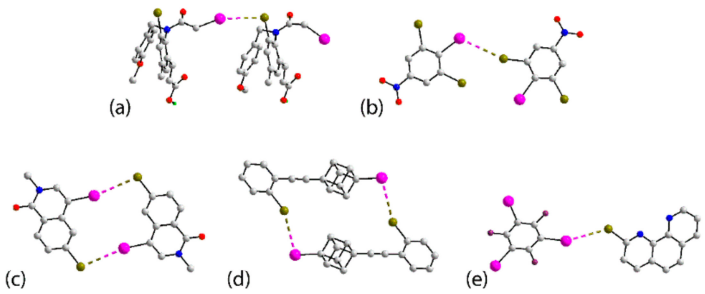

Figure 4. Zero-dimensional aggregates in the crystals of (**a**) **1**, (**b**) **3**, (**c**) **6**, (**d**) **7** and (**e**) co-crystal **9**. Additional colour code: nitrogen, blue; fluoride, plum; boron, teal.

3.2. One-Dimensional Aggregates Featuring I···Br Interactions

The most populous category among supramolecular architectures in this survey are supramolecular chains, having linear, zigzag and helical topologies. The chemical diagrams for the molecules in **10**–**39** forming the chains are shown in Figure 5. The chains present a rich diversity of bonding scenarios despite the relative simplicity of the supramolecular aggregation patterns.

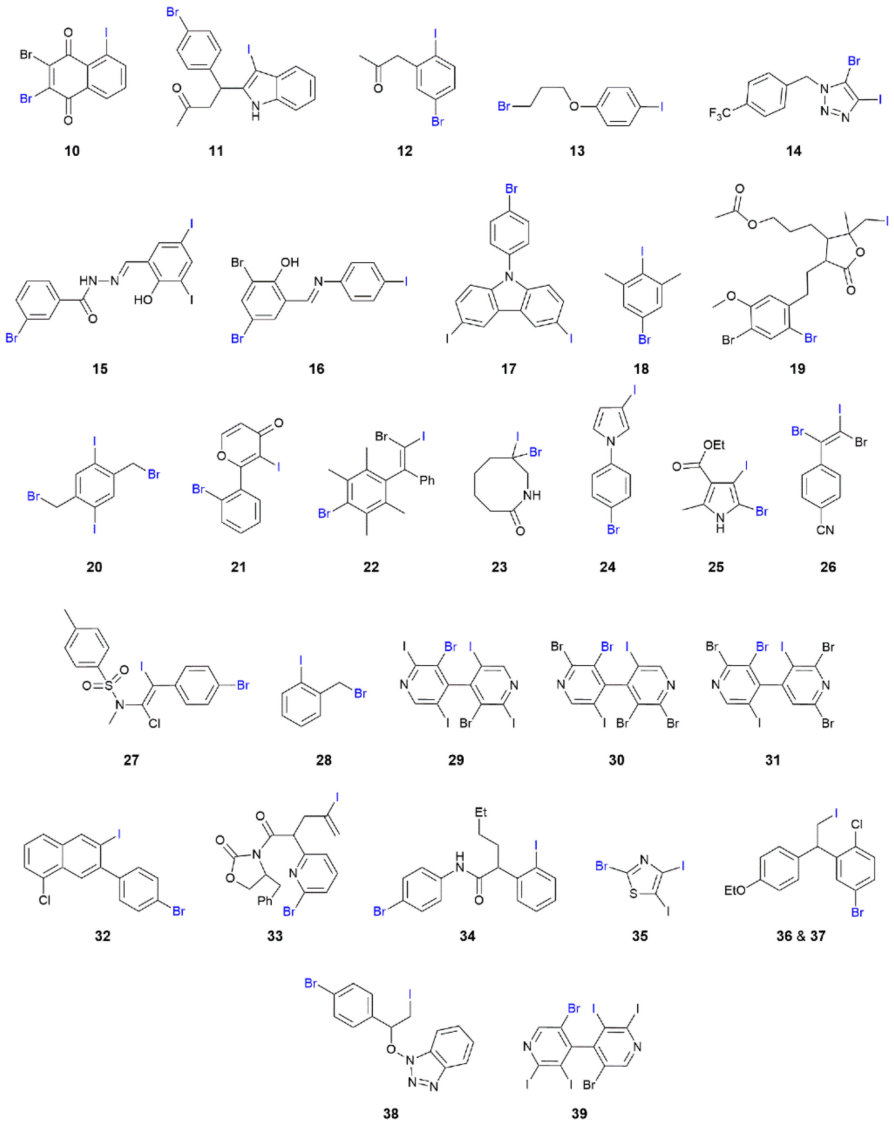

Figure 5. Chemical diagrams for molecules that form I···Br interactions in their crystals, leading to one-dimensional aggregation patterns (**10**–**39**).

Attention is first directed to analysing the linear chains. The prototype assembly with iodide functioning as the electrophile is illustrated in Figure 6a for **10** [50]. The chains in crystals of **11** [51] and **16** [56] follow the same trend in terms of bonding. On the other hand, chains with the bromide atom operating as the electrophile are evident in crystals of **14** [54], Figure 6b, and **19** [59].

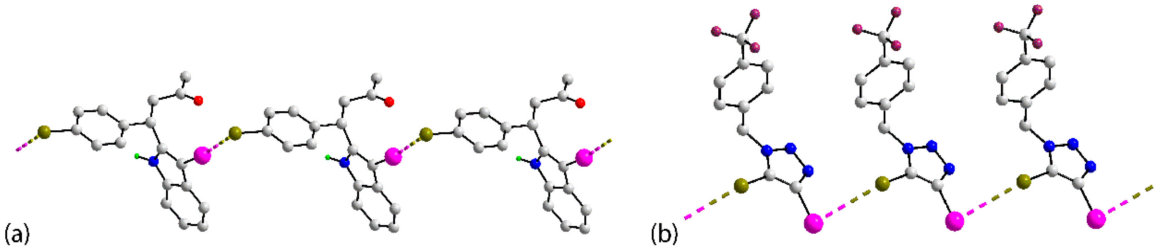

Figure 6. One-dimensional, linear chains in the crystals of (**a**) **10** and (**b**) **14**.

It was noted above for the zero-dimensional aggregate formed in co-crystal **9** that the magnitudes of the C–I···Br and C–Br···I angles were not greatly dissimilar. This observation is evident from the data collated in Table 1 for **12** [52], where the angles differ by less than 1°, Figure 7a, **13** [53], **15** [55], **17** [57] and **18** [58]; three independent molecules comprise the asymmetric unit of **18** and two of these self-assemble into a linear chain. The approximate linearity and near equivalence of the C–I···Br and C–Br···I angles rule out halogen bonding via a type-II interaction; it is likely these contacts have significant dispersion contributions (see below). A variation to the above is noted in the linear chain formed in the crystal of **20** [60]. Here, the two iodide and two bromide atoms of the centrosymmetric molecule engage in I···Br interactions, with the iodide being the electrophilic centre. The result is the formation of 10–membered $\{\cdots IC_3Br\}_2$ synthons and a linear tape, as highlighted in Figure 7b.

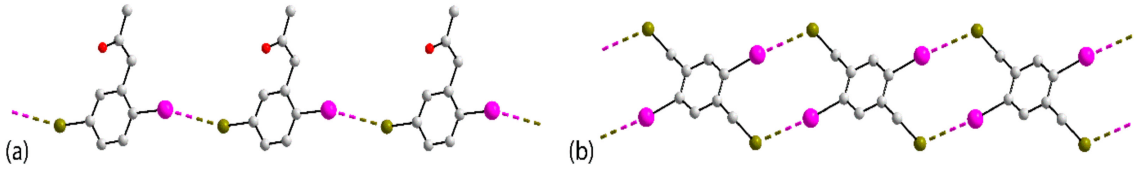

Figure 7. One-dimensional, linear chains in the crystals of (**a**) **12** and (**b**) **20**.

The next series of one-dimensional chains has I···Br interactions within a zigzag topology, as found in the crystals of **21** [61], **22** [62], **23** [63], **24** [64], **25** [65] and **26** [66]. The common crystallographic features of the solvent-free crystals, with the exception of **25**, are the presence of a single molecule in the asymmetric unit and the generation of the zigzag chain by glide symmetry. In **25**, the two independent molecules associate into a two-molecule aggregate with the chain propagated by glide symmetry. The crystals of **21**, **22**, Figure 8a, and **23** feature electrophilic iodide atoms. The remaining zigzag chains, that is, in crystals **24** [64], **25** [65] and **26** [66], do not exhibit great differences between the C–I···Br and C–Br···I angles, with the former being the wider only in the case of **24**; the chain in **26** is shown in Figure 8b.

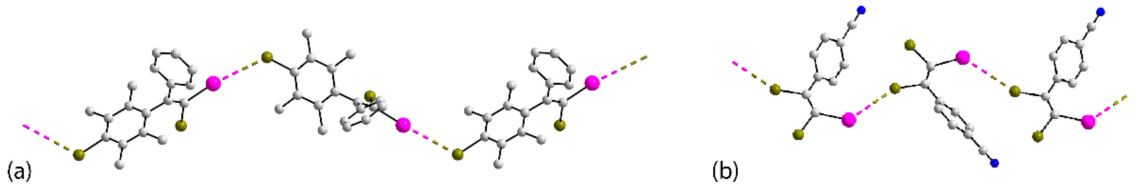

Figure 8. One-dimensional, zigzag chains in the crystals of (**a**) **22** and (**b**) **26**.

Comprising the largest subset of one-dimensional assembles, the are 13 crystals featuring helical chains, namely **27** [66], **28** [67], **29-31** [68], **32** [69], **33** [70], **34** [71], **35** [72], **36**, **37** [73], **38** [74] and **39** [68]. A high degree of homogeneity again exists among the solvent-free crystals with all helical chains being propagated by 2_1 screw symmetry. All but one crystal comprises a single molecule in the asymmetric unit. The exceptional crystal is **32**, where only one of the two independent molecules comprising the asymmetric unit

forms I···Br interactions and assembles into a helical chain. The chain formed in **27**, Figure 9a, is noteworthy for the relatively large number of heteroatoms available for interaction, whereas **28**, Table S1, is notable for its simplicity; both chains feature electrophilic iodide in accord with expectation. The variously substituted bipyridyl derivatives, **29**–**31** and **39**, are isostructural and form similar chains despite those in the crystals of **29** and **30** featuring electrophilic bromide and those in **31**, Figure 9b, and **39** having an electrophilic iodide. The remaining seven crystals are almost evenly divided between electrophilic iodide, namely **32**, **34** and **38**, and electrophilic bromide, namely **33**, Figure 9c, **35** and stereoisomers **36** and **37**.

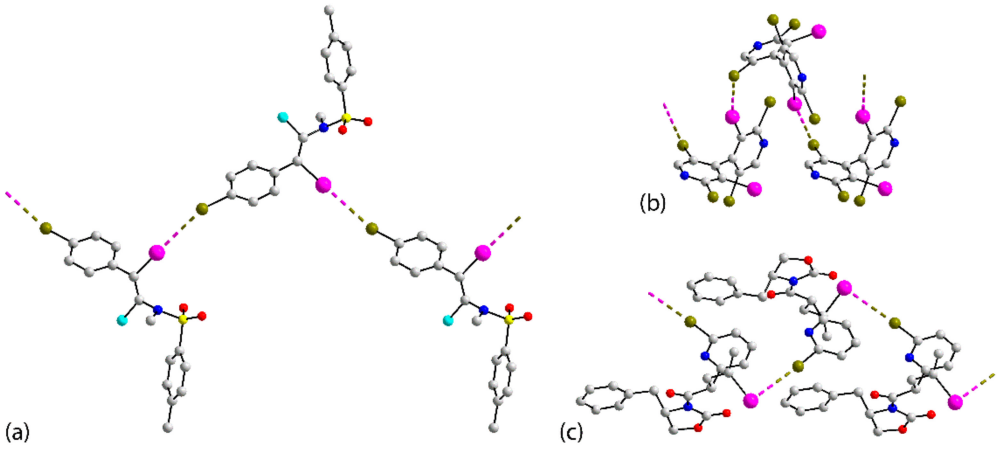

Figure 9. One-dimensional, helical chains in the crystals of (**a**) **27**, (**b**) **31** and (**c**) **33**.

3.3. Two- and Three-Dimensional Architectures Featuring I···Br Interactions

The two remaining crystals featuring I···Br interactions adopt either a two-dimensional array in the case of **40** [75] or a three-dimensional architecture as in the crystal of **41** [68]; the crystals are solvent-free. The chemical diagrams for **40** and **41** are given in Figure 10.

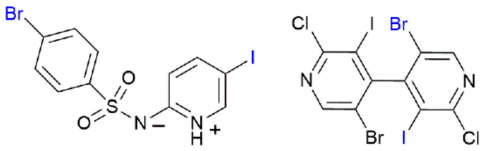

40 **41**

Figure 10. Chemical diagrams for molecules that form I···Br interactions in their crystals leading to two- and three-dimensional aggregation patterns (**40** and **41**).

An unprecedented mode of association mediated by I···Br interactions is found in the crystal of **40**, Figure 11. Here, both the iodide and bromide atoms form two I···Br interactions at right angles, indicating each atom functions as an electrophile and nucleophile simultaneously. As the halide atoms occupy positions at the extreme ends of the molecule, the I···Br interactions define zigzag chains, and a two-dimensional array with a flat topology is formed. Within the array featuring prominent zigzag chains of type-II halogen bonding, evidence for reinforcing S=O···π(arene) contacts is apparent, as detailed in Supplementary Materials, Table S1.

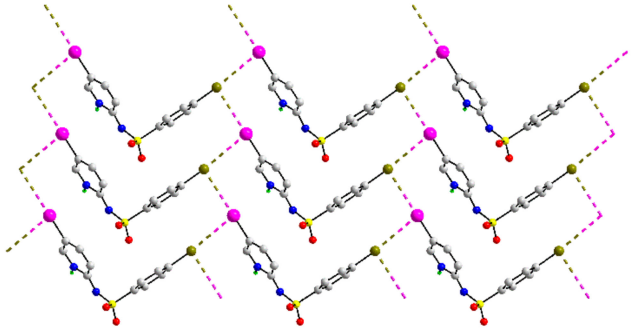

Figure 11. A view of the two-dimensional array in the crystal of **40**.

The molecule in **41** is related to several molecules found to form helical chains in their crystals, that is, **29**–**31** and **39**, see Figure 9b. Here, by contrast to the earlier examples, both iodide atoms participate in I···Br contacts but only one of the bromide atoms, which forms two interactions, providing a bridge. While helical chains are apparent, these are linked by the second set of I···Br interactions into a three-dimensional assembly, as represented in Figure 12.

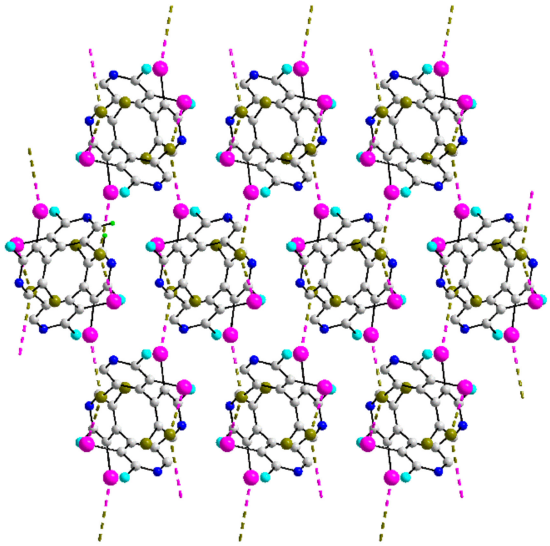

Figure 12. A view of the three-dimensional array in the crystal of **41**.

4. Relation to Congeners

The second component of the present analysis involves the evaluation of the propensity of X···X′ formation in direct congeners of **1**–**41**. To accomplish this, the CSD was evaluated for the presence of structures analogous to **1**–**41**, where any halides present in those molecules, participating in I···Br contacts or otherwise, were allowed to be any of fluoride, chloride, bromide and iodide. After removing molecules exhibiting disorder which could impact upon the supramolecular association, there were 11 sets of congeners. While the majority of the structures had one or two congeners only, several had more than that, with the subset of congeners related to **29** numbering an impressive 14 congeners (including **30**, **31**, **39** and **41**). Structural details for the congeners are included in Supplementary Materials, Table S2.

Five structures, namely **2**, **9**, **14**, **18** and **23**, each had a single congener. In the congener of **2** [42], where the bromide in the di-substituted phenyl—that is, not participating in the I···Br contact—is replaced by chloride, the I···Br interaction persists, leading to a two-molecule aggregate featuring a single contact but at the limit of the van der Waals radii. In the isostructural congener of co-crystal **9**, where the 1,10-phenanthroline-bound bromide was replaced by a chloride [49], an equivalent I···Cl contact is formed within the two-

molecule aggregate. The positions of the iodide and bromide atoms were interchanged in the congener of **14** [82], and while the molecules are orientated to form a linear chain as for **14**, the I···Br separation is beyond the van der Waals limit. Similarly, the bromide/iodide isomer of **18** lacks I···Br interactions [83]. The only congener of **23** is the isostructural all-iodide derivative, and an equivalent zigzag chain features I···I interactions [63].

The congeners reported for **3** do not have isostructural relationships in terms of space group symmetry and unit-cell characteristics. The congeners are the all-bromide [43] and all-chloride [84] derivatives and these present Br···Br and Cl···Cl contacts, respectively, to generate a two-molecule aggregate akin to that in the crystal of **3**. By contrast, strict isostructural relationships are apparent for most of the congeners of **20** and **21**. There are three congeners for **20**. In the first, the bromide atoms were replaced by chloride, and in the isostructural crystal, the chain features I···Cl interactions [60]. In the isostructural all-bromide congener [85], Br···Br contacts are apparent, see Table S2. Apparent are longer Br···Br contacts beyond the sum of the van der Waals radii. There is a polymorph of the isostructural all-bromide congener [85] in which each independent Br···Br interaction identified in the isostructural crystal now occurs at separations less than the sum of the van der Waals radii, resulting in a two-dimensional array with a distinctive zigzag topology, as represented in the plan view of Figure 13. In the case of **21**, the iodide atom was replaced by bromide in both known congeners and in one of these, the phenyl-bound bromide was substituted by chloride [61]. The isostructural crystals feature Br···Br and Br···Cl interactions within zigzag chains.

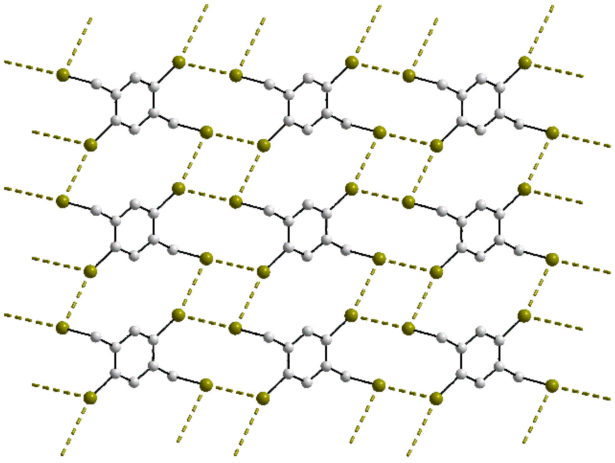

Figure 13. A view of the two-dimensional array in the crystal of a polymorph of the all-bromide congener of **20** (see text).

A complete series of isostructural crystals is known for the congeners of **40**. Thus, crystals with the four-position of the phenyl ring occupied by iodide, bromide, chloride and fluoride are available [75]. Here, each of the halides participate in a zigzag chain comprising I···X interactions. In the chloride congener, **40**_Cl, one I···Cl is equivalent to the sum of the van der Waals radii, while for the fluoride congener, **40**_F, both I···F separations are longer than the sum of the van der Waals radii (3.45 Å)—these structures are included for completeness of the discussion.

The availability of several series of isostructural crystals prompted an evaluation of the geometric parameters defining the X···X′ interactions. The analysis was restricted to crystal structure determinations carried out under the same experimental conditions in order to ensure, as much as possible, a valid comparison between the derived data for each series [86,87].

The geometric data for the X···X′ interactions in the four series of isostructural structures discussed up until now are collated in Table 2. An evaluation of the data enables the identification of several salient observations among the data. In the three series of

structures based on **20**, **21** and **23**, the heavier halide is always functioning as the electrophile, in accordance with expectation. Further, as judged by the percentages calculated for $[d(X\cdots X)/\sum vdW]$, relative to the van der Waals radii, interactions involving the heavier halide are relatively shorter. No apparent correlations are noted between the $d(X\cdots X)$ and either of C–X$\cdots$X′ and C–X′$\cdots$X. There is also a lack of clear correlation amongst the data assembled for congeners of **40**; the % $[d(X\cdots X)/\sum vdW]$ data for one interaction in **40**_Cl (100%) and both interactions in **40**_F (>100%) indicate these contacts are at or beyond the sums of the van der Waals radii, respectively. The lack of correlation in $d(I\cdots X')$ is seen, for example, in the type-II contacts involving the longer of the I$\cdots$X′ separations when X′ = I and F, but the shorter I$\cdots$X′ contacts when X′ is Br and Cl. However, there is a systematic decrease in the magnitude of the C–I$\cdots$X′ angles, passing from iodide to fluoride, and a parallel relationship among the C–X′$\cdots$I angles, although the latter trend is less convincing. In the same way, there are systematic decreases in the C–X′$\cdots$I and C–I$\cdots$X′ angles, respectively, for the type-II interactions formed by the X′ partner.

Table 2. Summary of geometric parameters (Å,°) in congeners of **20**, **21**, **23** and **40**.

Crystal	X	X′	d(X$\cdots$X′)	C–X$\cdots$X′ (θ_1)	C–X′$\cdots$X (θ_2)	%[d(X$\cdots$X)/ΣvdW] [a]	CSD REFCODE	Ref.
20	I	Br	3.6271(4)	166.66(7)	97.45(10)	94.7	MESMED	[60]
20_Cl	I	Cl	3.5373(9)	166.82(10)	99.27(14)	94.8	MESMIH	[60]
21	I	Br	3.6011(6)	175.22(11)	103.29(13)	94.0	YIZFUL	[61]
21_Br	Br	Br	3.5512(5)	175.86(9)	100.68(9)	96.0	YIZFOF	[61]
21_Cl	Br	Cl	3.4969(6)	174.70(6)	100.98(7)	97.1	YIZFIZ	[61]
23_I	I	I	3.7541(7)	173.90(16)	112.67(16)	94.8	SELYUE	[63]
23	I	Br	3.6666(12)	175.7(2)	115.3(2)	95.7	SELYOY	[63]
40_X = I	I	I	3.9277(8)	160.50(19)	88.39(19)	99.2	VEGSIL	[75]
			3.8761(9)	83.8(2)	175.2(2)	97.9		
40	I	Br	3.7436(5)	158.64(11)	87.49(12)	97.7	VEGSOR	[75]
			3.7465(6)	80.73(11)	172.51(12)	97.8		
40_X = Cl	I	Cl	3.6890(9)	156.80(8)	87.45(12)	98.9	VEGSUX	[75]
			3.7310(11)	78.73(8)	169.42(13)	100.0		
40_X = F	I	F	3.742(2)	152.21(9)	80.44(16)	109.5	VEGTAE	[75]
			3.512(3)	69.70(9)	159.44(19)	108.1		

[a] $\%[d(X\cdots X)/\sum vdW] = [d(X\cdots X)/\sum(van\ der\ Waals\ radii\ (X, X'))] \times 100$.

Next, attention is directed to the final two series of congeners, which also serve to highlight some of the observations above. There are six congeners for **16** and the chemical diagrams for these are given in Figure 14a. Three of the congeners, **16**_Br [88], **16**_I2 [89] and **16**_Cl [90], are isostructural, at least in terms of unit-cell symmetry. As for **16**, a linear chain occurs in the crystal of **16**_Br but features Br$\cdots$Br interactions. Despite the isostructural relationship, no X$\cdots$X′ contacts less than the van der Waals radii are apparent in the crystals of **16**_I2 and **16**_Cl. Nevertheless, if two independent X$\cdots$X′ contacts longer than the van der Waals radii are considered (see Table S2 for geometric details), supramolecular tapes are apparent, as shown for **16**_I2 in Table S2. No separations less than the van der Waals radii are noted in the crystals of **16**_Cl2 [91]. It is noted that long type-II Br$\cdots$Br and Br$\cdots$Cl interactions link molecules into a layer and these are connected into a three-dimensional array via long, type-II Cl$\cdots$Cl contacts. Details and images are given in Table S2. Short Br$\cdots$Br separations across a centre of inversion are apparent in the crystal of **16**_F [92], leading to the dimeric aggregate illustrated in Figure 14b. Finally, in **16**_FI [93], two independent molecules comprise the asymmetric unit, and one of these assembles into a zigzag chain (glide-symmetry) via type-II I$\cdots$I interactions, as shown in Figure 14c.

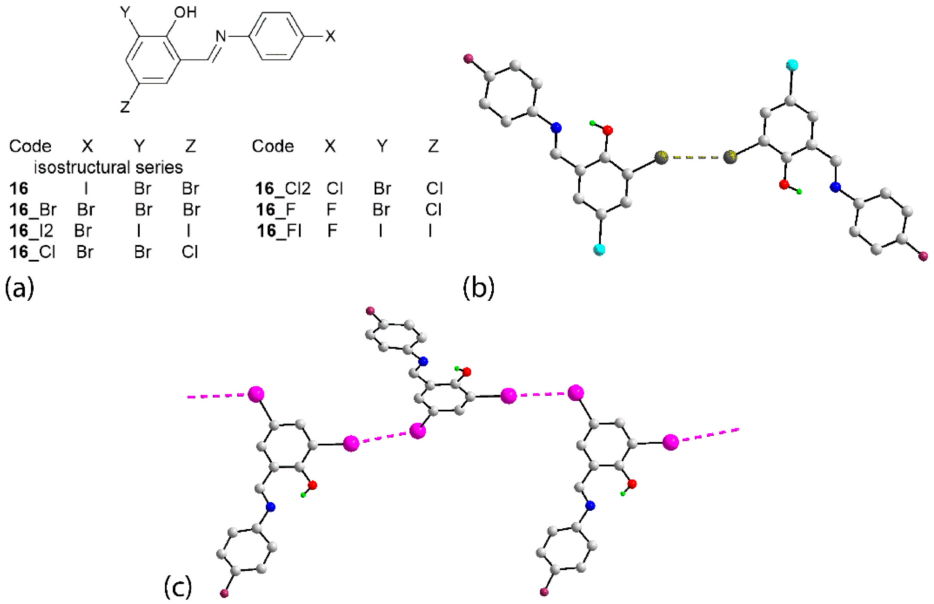

Figure 14. (**a**) Chemical diagrams for the congeners of **16**, (**b**) the centrosymmetric dimer in **16**_F (d(Br···Br) = 3.5526(9) Å; 2 × C–Br···Br = 140.32(10)°) and (**c**) a view of the zigzag, one-dimensional chain in the crystal of **16**_FI (d(I···I) = 3.7476(15) Å; C–I···I = 161.58(4)° and C–I···I = 109.34(4)°).

Arguably the most perplexing series of structures is noted for the set of hexahalogenated 4,4′-bipyridine congeners which are isostructural, crystallising solvent-free in the orthorhombic space group $P2_12_12_1$, $Z' = 1$ and with similar unit-cell parameters [68]; see Table S2 for details. The chemical diagrams and numbering scheme for the 14 congeners are given in Figure 15a. Five of the crystals feature I···Br interactions and were described above. Thus, **29**–**31** assemble into helical chains (2_1 screw symmetry) along the *a*-axis, **39** into a two-dimensional array and **41** into a three-dimensional framework. Indeed, this series is a microcosm for all the aggregates discussed in this survey, as three of the congeners are classified as isolated molecules based on the strict application of the van der Waals criterion. Compound **29**_1 does not feature any close X···X′ contacts but in **29**_2 and **29**_3, Br···Br (3.7441(15) Å) and I···Br (3.7327(17) Å) contacts a little beyond the sum of the van der Waals radii are found in the molecules related by 2_1 screw symmetry aligned along the *a*-axis. Helical chains are found in each of **30**_1, **30**_2, **30**_Br and **30**_I featuring I···Cl, Br···Br, Br···Br and I···I interactions, respectively. A two-dimensional array occurs in the crystal of **29**_4, Figure 15b. As noted by the authors of the original report [68], the molecule in **29**_4 was the outlier among the 14 congeners in terms of its conformation, with an almost orthogonal relationship between the pyridyl rings and the other molecules being relatively homogeneous. The characteristic helical chain occurs along the *a*-axis, as for most of the assemblies, and these feature type-II Br···Br interactions; see the caption to Figure 15 for the geometric parameters. These are linked into a two-dimensional array via I···Br interactions with geometric characteristics, indicating a bonding situation intermediate between type-I and type-II bonding. In this assembly, one bromide atom connects to both iodide and bromide while the other only participates in Br···Br interactions. The crystal of **41**_1 resembles closely the three-dimensional architecture illustrated for **41** in Figure 12, with the X···X′ contacts involving iodide atoms exclusively (Table S2).

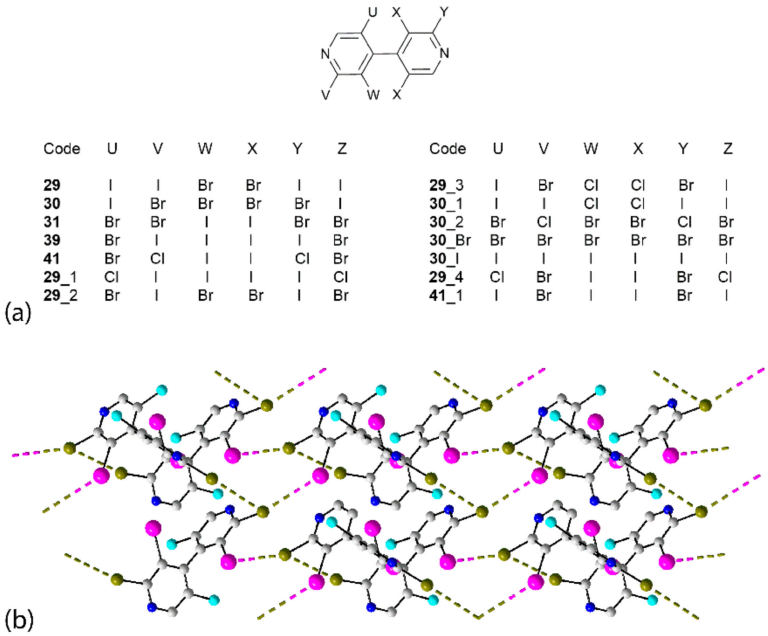

Code	U	V	W	X	Y	Z
29	I	I	Br	Br	I	I
30	I	Br	Br	Br	Br	I
31	Br	Br	I	I	Br	Br
39	Br	I	I	I	I	Br
41	Br	Cl	I	I	Cl	Br
29_1	Cl	I	I	I	I	Cl
29_2	Br	I	Br	Br	I	Br

Code	U	V	W	X	Y	Z
29_3	I	Br	Cl	Cl	Br	I
30_1	I	I	Cl	Cl	I	I
30_2	Br	Cl	Br	Br	Cl	Br
30_Br	Br	Br	Br	Br	Br	Br
30_I	I	I	I	I	I	I
29_4	Cl	Br	I	I	Br	Cl
41_1	I	Br	I	I	Br	I

Figure 15. (**a**) Chemical diagrams for the congeners of **29** and (**b**) a view of the two-dimensional array in the crystal of **29**_4 (d(Br· · · Br) = 3.565(2) Å; C–Br· · · Br = 165.29(11)° and C–Br· · · Br = 73.51(11)°) and (d(I· · · Br) = 3.749(2) Å; C–I· · · Br = 125.61(10)° and C–Br· · · I = 157.27(11)°).

5. Overview

In all, 41 crystals featured at least one I· · · Br interaction operating independently of other obvious intermolecular contacts and lacking additional X· · · X′ halogen bonding interactions in the crystal. In nine instances, these led to zero-dimensional aggregates, always comprising two molecules. There were 30 supramolecular chains with linear (11), zigzag (6) and helical (13) topologies. One crystal had a two-dimensional assembly featuring I· · · Br interactions and there was also a single example of a three-dimensional architecture featuring I· · · Br interactions. In the majority of crystals, the participating molecule I· · · Br interactions formed, on average, a single contact. However, there were three examples where, on average, the participating molecule formed half a contact (**1**–**3**). Conversely, there were two examples, that is, **40** and **41**, where there were two I· · · Br interactions per molecule.

Referring to Figure 2, in the present survey there were both type-I and type-II contacts between iodide and bromide. While for a type-I interaction, the values of θ_1 and θ_1 are anticipated to be close to each other and generally greater than 130°, in a type-II interaction, the values of θ_1 and θ_2 hover around 90 and 180°, respectively. From the foregoing survey of the aggregation patterns in **1**–**41** and the values tabulated in Table 1, there is a deviation from expectation for the type-II contacts, as commented upon above. When forming I· · · Br contacts, iodide might be expected to function as the electrophile and bromide to fulfil the role as nucleophile in accord with the greater polarizability of iodide with respect to bromide.

With reference to the data in Table 1, there are 45 independent I· · · Br contacts among the 41 structures; there are 41 if interactions where the iodide atom forms two contacts are ignored, as in crystals **40** and **41**. Type-I contacts, where the difference between θ_1 and θ_2 angles is less than 10°, are found for five interactions, in crystals **12**, **13**, **15** and **18**. A second group comprising eight interactions has a difference between θ_1 and θ_2 angles greater than 10° but less than 40°, as in crystals **5**, **9**, **17**, **24**, **25**, **26** and **27,** and might be considered an intermediate bonding situation between the type I and type II extremes. The remaining 28 I· · · Br interactions can be classified as type-II contacts. For these contacts, iodide functions as the electrophile in 16 of these, and bromide in 12 cases. For the three crystals featuring two contacts per iodide, the iodide atom is bifunctional, acting as both an electrophile

and a nucleophile at the same time. Clearly, further high-level computational chemistry is required in order to further understand the true nature of the bonding in these systems.

Keeping in mind that the discussion revolves around inherently weak intermolecular interactions and that the electronic nature of the halide can be readily moderated by the atoms forming the covalent bond to the halide, this observation of an interplay between electrophilic/nucleophilic roles for iodide and bromide is perhaps not so surprising.

While it is ingrained in the supramolecular chemistry community that when analysing intermolecular contacts correlations involving bond lengths and angles are always going to be challenging [94,95], it was thought of interest to ascertain any trends in the I···Br separations in the 28 examples where type-II halogen bonding interactions are evident. The average I···Br separation for all 28 examples computes to 3.716 Å. This is longer than the average value for type-II I···Br contacts with 3.690 Å and conversely, shorter than 3.752 Å, being the average for type-II Br···I contacts. It is noted there are almost overlapping ranges of the separations, that is, 3.540 to 3.814 Å and 3.564 to 3.813 Å for type-II I···Br and Br···I contacts, respectively. Based on this limited database of structures, and if shorter separations correspond to stronger interactions, type-II I···Br contacts tend to be stronger than their type-II Br···I analogues. A comment on the C–I···Br and C–Br···I angles for the type-II halogen bonding is also made, if nothing more than for the record. For the C–I···Br interactions, the average values of θ_1 and θ_2 were 169.2 and 77.4°, respectively; the ranges of θ_1 and θ_2 were 161.3 to 175.7° and 76.3 to 121.9°, respectively. The equivalent values for the C–Br···I angles were 159.6 and 103.4°, respectively; the ranges were 148.8 to 171.2° and 71.9 to 117.8°, respectively. These limited data tend to indicate type-II I···Br interactions are more linear than their type-II Br···I equivalents and angles greater than 175° are rare.

Next, an evaluation of the pervasiveness of I···Br interactions in **1**–**41** was undertaken. A search of the CSD was conducted for crystals containing both C–I and C–Br bonds. This returned 212 (uncorrected) hits. Therefore, unsupported I···Br interactions are found in over 22% of all crystals where this interaction can potentially form and where there are no other halogen bonding interactions at separations less than van der Waals distances. If the latter restriction is removed, the percentage adoption of I···Br halogen-bonds in crystals rises to at least 27% of all structures. This less than the 33% adoption rate of the $\{\cdots O{=}COH\}_2$ dimer synthon in organic crystals [96].

Of the 41 crystals, nine crystallised with multiple molecules in the asymmetric unit. While in **25**, each of the two independent molecules formed on average one I···Br interaction, this pattern was not repeated in the other eight crystals. In **2** and **3**, each with two independent molecules connected by a single I···Br interaction, indicates, on average, half of an I···Br interaction per molecule. A similar situation pertains in **1**, where two of the four independent molecules form, on average, half an interaction through dimer formation. In **18**, two of three independent molecules participate in comparable I···Br interactions. In each of **4**, **6**, **32** and **34**, only one of the two independent molecules forms I···Br interactions. This overview suggests there is no inherent propensity of molecules to form an I···Br interaction. In keeping with this conclusion, it is noted that 10 out of the 41 molecules included in the discussion herein feature two (9) or three (1) iodide atoms. Yet, only in the case of **41** were two iodide atoms engaged in the formation of I···Br contacts.

The persistence of the I···Br halogen bonding interactions was also evaluated in their structural congeners. Eleven of the 41 crystals had congeners resulting in another 30 crystals for analysis. Generally, when heavier iodide and bromide were present in the congeners, related X···X′ halogen bonding interactions giving similar supramolecular aggregation patterns were observed, but not always so, such as in instances where separations were longer than the sum of the respective van der Waals radii, for example, in the congeners of **2** and **18**. When the halide was lighter, as in chloride and fluoride, in accordance with expectation, the X···X′ interactions were less likely to persist, for example, in the congeners of **3**.

Seven of the congeners exhibited strict isostructural relationships in terms of space group symmetry. Even then, several anticipated X···X′ interactions were beyond the van der Waals radii, sometimes at relatively great separations. In some of the series, different aggregation patterns were apparent despite the isostructural relationships, most notably for the congeners of **16** and **29**. This observation is particularly true for the latter series where a full range of aggregation patterns, namely, none, zero-, one-, two- and three-dimensional, based on X···X′ halogen bonding was noted. This observation invites the possibility of the scenario where molecule crystals condense from solution and optimise all possible intermolecular contacts to establish the most stable crystalline manifold, which may not necessarily include all or even some of the possible X···X′ interactions.

Consistent with the abovementioned information, systematic variations in geometric parameters were not generally apparent, even among isostructural series; some evidence for increasing strength of X···X′ interactions, following the order I > Br > Cl > F, was noted see Table 2. The axiom concerning detecting trends in intermolecular interactions, which are inherently weak, notwithstanding [94,95], might have anticipated that with isostructural relationships existing in several series where there was the adoption of a common aggregation pattern along with consistent type-II halogen bonding, such correlations might be possible. However, this was not the case.

6. Conclusions

The presence of standalone I···Br interactions in crystals devoid of other halogen bonding has been established in over 22% of instances where these can occur. A range of supramolecular aggregation patterns feature these interactions, with the majority (75%) being supramolecular chains. Similarly, a full range of bonding possibilities are evident, including type-I, type-II and in between. When type-II bonding was apparent, the participating σ–hole was implied to reside on the iodide in approximately two-thirds of the cases, with one-third involving the σ–hole of the bromide atom. Sophisticated computational chemistry will be required to resolve this issue, but these observations point to a high degree of flexibility in the formation of I···Br interactions. An investigation of the presence of congeners revealed over a quarter of the identified crystals have congeners, with the majority having at least one isostructural mate. While the establishment of isostructural relationships is encouraging and offers the opportunity of fine tuning in terms of tailoring properties of crystals, in many cases distinct aggregation patterns were noted. This implied whatever the strength and directionality of X···X′ interactions, these are subject to other imperatives during the crystallisation process, the most obvious and perhaps most difficult being global molecular packing considerations. Clearly, this is a fertile area in crystal engineering worthy of further detailed investigation, which would only benefit from controlled crystallisation experiments with supporting computational chemistry.

Supplementary Materials: The following are available online at https://www.mdpi.com/article/10.3390/cryst11040433/s1, Table S1: Details of composition, images and geometric details in crystals featuring I···Br interactions in **1**–**41** and Table S2: Details of composition, images, unit-cell details and geometric details in congener crystals featuring putative X···X interactions.

Funding: This research was funded by Sunway University Sdn Bhd, grant number GRTIN-IRG-01-2021.

Data Availability Statement: Not applicable.

Conflicts of Interest: The author declares no conflict of interest.

References

1. Hassel, O.; Hvoslef, J. The Structure of Bromine 1,4-Dioxanate. *Acta Chem. Scand.* **1954**, *8*, 873. [CrossRef]
2. Spek, A.L. CheckCIF Validation ALERTS: What They Mean and How to Respond. *Acta Crystallogr. Sect. E Crystallogr. Commun.* **2020**, *76*, 1–11. [CrossRef]
3. Alcock, N.W. Secondary Bonding to Nonmetallic Elements. *Adv. Inorg. Chem. Radiochem.* **1972**, *15*, 1–58. [CrossRef]
4. Mulliken, R.S. Structures of Complexes Formed by Halogen Molecules with Aromatic and with Oxygenated Solvents. *J. Am. Chem. Soc.* **1950**, *72*, 600–608. [CrossRef]

5. Bent, H.A. Structural Chemistry of Donor-Acceptor Interactions. *Chem. Rev.* **1968**, *68*, 587–648. [CrossRef]
6. Hassel, O. Structural Aspects of Interatomic Charge-Transfer Bonding. *Science* **1970**, *170*, 497–502. [CrossRef]
7. Colin, M.M.; Gaultier de Claubry, H. Sur le Combinaisons de l'iode Avec les Substances Végétales et Animales. *Ann. Chim.* **1814**, *90*, 87–100.
8. Guthrie, F. On the Iodide of Iodammonium. *J. Chem. Soc.* **1863**, *16*, 239–244. [CrossRef]
9. Clark, T.; Hennemann, M.; Murray, J.S.; Politzer, P. Halogen Bonding: The Sigma-Hole. *J. Mol. Model.* **2007**, *13*, 291–296. [CrossRef]
10. Kolář, M.H.; Hobza, P. Computer Modeling of Halogen Bonds and Other σ-hole Interactions. *Chem. Rev.* **2016**, *116*, 5155–5187. [CrossRef]
11. Politzer, P.; Murray, J.S. σ-Hole Interactions: Perspectives and Misconceptions. *Crystals* **2017**, *7*, 212. [CrossRef]
12. Metrangolo, P.; Neukirch, H.; Pilati, T.; Resnati, G. Halogen Bonding Based Recognition Processes: A world Parallel to Hydrogen Bonding. *Acc. Chem. Res.* **2005**, *38*, 386–395. [CrossRef]
13. Mukherjee, A.; Tothadi, S.; Desiraju, G.R. Halogen Bonds in Crystal Engineering: Like Hydrogen bonds Yet Different. *Acc. Chem. Res.* **2014**, *47*, 2514–2524. [CrossRef]
14. Crabtree, R.H. Hypervalency, Secondary Bonding and Hydrogen Bonding: Siblings under the Skin. *Chem. Soc. Rev.* **2017**, *46*, 1720–1729. [CrossRef] [PubMed]
15. Riel, A.M.S.; Rowe, R.K.; Ho, E.N.; Carlsson, A.-C.C.; Rappé, A.K.; Berryman, O.B.; Ho, P.S. Hydrogen Bond Enhanced Halogen Bonds: A Synergistic Interaction in Chemistry and Biochemistry. *Acc. Chem. Res.* **2019**, *52*, 2870–2880. [CrossRef]
16. Gilday, L.C.; Robinson, S.W.; Barendt, T.A.; Langton, M.J.; Mullaney, B.R.; Beer, P.D. Halogen Bonding in Supramolecular Chemistry. *Chem. Rev.* **2015**, *115*, 7118–7195. [CrossRef]
17. Christopherson, J.-C.; Topić, F.; Barrett, C.J.; Friščic, T. Halogen-Bonded Cocrystals as Optical Materials: Next-Generation Control over Light−Matter Interactions. *Cryst. Growth Des.* **2018**, *18*, 1245–1259. [CrossRef]
18. Pancholi, J.; Beer, P.D. Halogen Bonding Motifs for Anion Recognition. *Coord. Chem. Rev.* **2020**, *416*, 213281. [CrossRef]
19. Saccone, M.; Catalano, L. Halogen Bonding beyond Crystals in Materials Science. *J. Phys. Chem. B* **2019**, *123*, 9281–9290. [CrossRef] [PubMed]
20. Beale, T.M.; Chudzinski, M.G.; Sarwar, M.G.; Taylor, M.S. Halogen Bonding in Solution: Thermodynamics and Applications. *Chem. Soc. Rev.* **2013**, *42*, 1667–1690. [CrossRef]
21. Tepper, R.; Schubert, U.S. Halogen Bonding in Solution: Anion Recognition, Templated Self-Assembly, and Organocatalysis. *Angew. Chem. Int. Ed.* **2018**, *57*, 6004–6016. [CrossRef] [PubMed]
22. Von der Heiden, D.; Vanderkooy, A.; Erdélyi, M. Halogen Bonding in Solution: NMR Spectroscopic Approaches. *Coord. Chem. Rev.* **2020**, *407*, 213147. [CrossRef]
23. Parisini, E.; Metrangolo, P.; Pilati, T.; Resnati, G.; Terraneo, G. Halogen Bonding in Halocarbon–Protein Complexes: A Structural Survey. *Chem. Soc. Rev.* **2011**, *40*, 2267–2278. [CrossRef] [PubMed]
24. Scholfield, M.R.; Vander Zanden, C.M.; Carter, M.; Ho, P.S. Halogen Bonding (X-Bonding): A Biological Perspective. *Prot. Sci.* **2013**, *22*, 139–152. [CrossRef] [PubMed]
25. Brammer, L.; Espallargas, G.M.; Libri, S. Combining Metals with Halogen Bonds. *CrystEngComm* **2008**, *10*, 1712–1727. [CrossRef]
26. Mosquera, M.E.G.; Egido, I.; Hortelano, C.; López-López, M.; Gómez-Sal, P. Comparison of Halogen Bonding Networks with Ru(II) Complexes and Analysis of the Influence of the XB Interactions on Their Reactivity. *Faraday Discuss.* **2017**, *203*, 257–283. [CrossRef]
27. Adonin, S.A.; Sokolov, M.N.; Fedin, V.P. Polyhalide-Bonded Metal Complexes: Structural Diversity in an Eclectic Class of Compounds. *Coord. Chem. Rev.* **2018**, *367*, 1–17. [CrossRef]
28. Fourmigué, M. Halogen Bonding: Recent Advances. *Curr. Opin. Solid State Mater. Sci.* **2009**, *13*, 36–45. [CrossRef]
29. Cavallo, G.; Metrangolo, P.; Milani, R.; Pilati, T.; Priimagi, A.; Resnati, G.; Terraneo, G. The Halogen Bond. *Chem. Rev.* **2016**, *116*, 2478–2601. [CrossRef]
30. Liu, Y.; Tiekink, E.R.T. Supramolecular Associations in Binary Antimony(III) Dithiocarbamates: Influence of Ligand Steric Bulk, Influence on Coordination Geometry, and Competition with Hydrogen Bonding. *CrystEngComm* **2005**, *7*, 20–27. [CrossRef]
31. Tiekink, E.R.T. Aggregation Patterns in the Crystal Structures of Organometallic Group XV 1,1-Dithiolates: The Influence of the Lewis Acidity of the Central Atom, Metal- and Ligand-Bound Steric Bulk, and Coordination Potential of the 1,1-Dithiolate Ligands upon Supramolecular Architecture. *CrystEngComm* **2006**, *8*, 104–118. [CrossRef]
32. Lai, C.S.; Tiekink, E.R.T. Prevalence of Intermolecular Bi···S Interactions in Bismuth Dithiocarbamate Compounds: $Bi(S_2CNR_2)_3$. *Z. Kristallogr.* **2007**, *222*, 532–538. [CrossRef]
33. Tiekink, E.R.T.; Zukerman-Schpector, J. Stereochemical Activity of Lone Pairs of Electrons and Supramolecular Aggregation Patterns Based on Secondary Interactions Involving Tellurium in Its 1,1-Dithiolate Structures. *Coord. Chem. Rev.* **2010**, *254*, 46–76. [CrossRef]
34. Lee, S.M.; Heard, P.J.; Tiekink, E.R.T. Molecular and Supramolecular Chemistry of Mono- and Di-Selenium Analogues of Metal Dithiocarbamates. *Coord. Chem. Rev.* **2018**, *375*, 410–423. [CrossRef]
35. Tiekink, E.R.T. A Survey of Supramolecular Aggregation Based on Main Group Element···Selenium Secondary Bonding Interactions – A Survey of the Crystallographic Literature. *Crystals* **2020**, *10*, 503. [CrossRef]
36. Tiekink, E.R.T. Zero-, One-, Two- and Three-Dimensional Supramolecular Architectures Sustained by Se···O Chalcogen Bonding: A Crystallographic Survey. *Coord. Chem. Rev.* **2021**, *427*, 213586. [CrossRef]

37. Tiekink, E.R.T. Supramolecular Architectures Sustained by Delocalised C–I$\cdots\pi$(Arene) Interactions in Molecular Crystals and the Propensity of Their Formation. *CrystEngComm* **2021**, *23*, 904–928. [CrossRef]
38. Taylor, R.; Wood, P.A. A Million Crystal Structures: The Whole is Greater than the Sum of Its Parts. *Chem. Rev.* **2019**, *119*, 9427–9477. [CrossRef] [PubMed]
39. Bruno, I.J.; Cole, J.C.; Edgington, P.R.; Kessler, M.; Macrae, C.F.; McCabe, P.; Pearson, J.; Taylor, R. New Software for Searching the Cambridge Structural Database and Visualizing Crystal Structures. *Acta Crystallogr. Sect. B Struct. Sci. Cryst. Eng. Mater.* **2002**, *58*, 389–397. [CrossRef]
40. Brandenburg, K.; Berndt, M. *DIAMOND, Version 3.2k*; GbR: Bonn, Germany, 2006.
41. Guthrie, D.B.; Geib, S.J.; Curran, D.P. Synthesis of Highly Enantioenriched 3,4-Dihydroquinolin-2-Ones by 6-Exo-Trig Radical Cyclizations of Axially Chiral α-Halo-Ortho-Alkenyl Anilides. *J. Am. Chem. Soc.* **2009**, *131*, 15492–15500. [CrossRef]
42. Leroux, F.R.; Berthelot, A.; Bonnafoux, L.; Panossian, A.; Colobert, F. Transition-Metal-Free Atropo-Selective Synthesis of Biaryl Compounds Based on Arynes. *Chem.-Eur. J.* **2012**, *18*, 14232–14236. [CrossRef] [PubMed]
43. Romero, J.A.; Aguirre Hernández, G.; Bernès, S. Anomalous Halogen Bonds in the Crystal Structures of 1,2,3-TriBromo-5-Nitro-Benzene and 1,3-DiBromo-2-Iodo-5-NitroBenzene. *Acta Crystallogr., Sect. E: Cryst. Commun.* **2015**, *71*, 960–965. [CrossRef]
44. Franz, A.K.; Dreyfuss, P.D.; Schreiber, S.L. Synthesis and Cellular Profiling of Diverse Organosilicon Small Molecules. *J. Am. Chem. Soc.* **2007**, *129*, 1020–1021. [CrossRef] [PubMed]
45. Qiu, L.; Wang, D.; Lv, F.; Guo, X.; Hu, W.; Yang, L.; Liu, S. Three-Component Reactions Based on Trapping Ammonium Ylides with N-Sulfonyl Aldimines via Cooperative Catalysis of Squaramides and $Rh_2(OAc)_4$. *Tetrahedron* **2014**, *70*, 1471–1477. [CrossRef]
46. Fang, Z.; Wang, Y.; Wang, Y. Synthesis of 4-Iodoisoquinolin-1(2H)-Ones by a Dirhodium(II)-Catalyzed 1,4-Bisfunctionalization of Isoquinolinium Iodide Salts. *Org. Lett.* **2019**, *21*, 434–438. [CrossRef] [PubMed]
47. Flanagan, K.; Bernhard, S.S.R.; Plunkett, S.; Senge, M.O. Not Your Usual Bioisosteres: Solid State Study of 3D Interactions in Cubanes. *Chem. Eur. J.* **2019**, *25*, 6941–6954. [CrossRef]
48. Messaoud, M.Y.A.; Bentabed-Ababsa, G.; Hedidi, M.; Derdour, A.; Chevallier, F.; Halauko, Y.S.; Ivashkevich, O.A.; Matulis, V.E.; Picot, L.; Thiéry, V.; et al. Deproto-Metallation of N-Arylated Pyrroles and Indoles Using a Mixed Lithium–Zinc Base and Regioselectivity-Computed CH Acidity Relationship. *Beilstein J. Org. Chem.* **2015**, *11*, 1475–1485. [CrossRef] [PubMed]
49. Zhang, Y.; Wang, J.G.; Wang, W. Noncovalent Interactions Between 1,3,5-Trifluoro-2,4,6-Triiodobenzene and a Series of 1,10-Phenanthroline Derivatives: A Combined Theoretical and Experimental Study. *Crystals* **2019**, *9*, 140. [CrossRef]
50. Hong, L.; Sun, W.; Liu, C.; Wang, L.; Wong, K.; Wang, R. Enantioselective Friedel–Crafts Alkylation of 4,7-Dihydroindoles with Enones Catalyzed by Primary–Secondary Diamines. *Chem. Eur. J.* **2009**, *15*, 11105–11108. [CrossRef] [PubMed]
51. Jardim, G.A.M.; da Silva Júnior, E.N.; Bower, J.F. Overcoming Naphthoquinone Deactivation: Rhodium-Catalyzed C-5 Selective C–H Iodination as A Gateway to Functionalized Derivatives. *Chem. Sci.* **2016**, *7*, 3780–3784. [CrossRef] [PubMed]
52. Bian, H.L.; Tang, S.Z.; Chen, M.E.; Zhang, X.M.; Lv, J.W.; Chen, X.W.; Qi, F.M.; Chen, S.W.; Zhang, F.M. Transition-Metal-Free site-Selective γ-C(sp^2)–H Monoiodination of Arenes Directed by an Aliphatic Keto Group. *Org. Lett.* **2020**, *22*, 5314–5319. [CrossRef] [PubMed]
53. Wu, Z.; Liu, X.; Shen, P.; Jiang, S. 1-(3-Bromopropoxy)-4-Iodobenzene. *Acta Crystallogr. Sect. E Struct. Rep. Online* **2007**, *63*, o4760. [CrossRef]
54. Rheingold, A.L. Private Communication to the Cambridge Structural Database. *Refcode CORZER* **2019**. [CrossRef]
55. Ning, J.H.; Xu, X.W. 3-Bromo-N′-(2-Hydroxy-3,5-Diiodobenzylidene)benzohydrazide Monohydrate. *Acta Crystallogr. Sect. E Struct. Rep. Online* **2009**, *65*, o905–o906. [CrossRef] [PubMed]
56. Guo, M.L.; Nong, X.R.; Yin, H. 2,4-Dibromo-6-(4-IodoPhenylIminoMethyl)Phenol. *Acta Crystallogr. Sect. E: Struct. Rep. Online* **2007**, *63*, o4640. [CrossRef]
57. Tang, G.M.; Chi, R.H.; Wan, W.Z.; Wang, Y.T.; Cui, Y.Z.; Ng, S.W. Synthesis, Crystal Structures, and Nonlinear Optic and Thermal Properties of Two Diiodocarbazole Derivatives. *J. Chem. Res.* **2017**, *41*, 79–81. [CrossRef]
58. Liu, R.; Li, Y.H.; Luo, W.; Liu, S.; Zhu, H.J. 5-Bromo-2-Iodo-1,3-Dimethylbenzene. *Acta Crystallogr. Sect. E Struct. Rep. Online* **2008**, *64*, o219. [CrossRef] [PubMed]
59. Kaluza, N.M.; Schollmeyer, D.; Nubbemeyer, U. Total Synthesis of (–)-C/D-Cis-DeHydro-3-O-Methyl-Estradiols. *Eur. J. Org. Chem.* **2016**, *2*, 357–366. [CrossRef]
60. Gaefke, G.; Enkelmann, V.; Höger, S. A Practical Synthesis of 1,4-Diiodo-2,5-Bis(chloromethyl)benzene and 1,4-Diiodo-2,5-Bis(bromomethyl)benzene. *Synthesis* **2006**, *17*, 2971–2973. [CrossRef]
61. Gholap, S.P.; Jangid, D.; Fernandes, R.A. Metal-Free Brønsted Acid-Catalyzed Rearrangement of δ-Hydroxyalkynones to 2,3-Dihydro-4H-Pyran-4-Ones: Total Synthesis of Obolactone and a Catechol Pyran Isolated from *Plectranthus Sylvestris*. *J. Org. Chem.* **2019**, *84*, 3537–3551. [CrossRef] [PubMed]
62. Maji, B.; Bhattacharya, A.; Hazra, S. Halogen-Induced Friedel-Crafts Alkenylation Reactions with Haloalkynes: Direct Access to Gem-1, 1-Dihaloalkenes. *Chem. Sel.* **2017**, *2*, 10375–10378. [CrossRef]
63. Hu, T.; Shen, M.; Chen, Q.; Li, C. Pushing Radical Cyclization from Regioselective to Regiospecific: Cyclization of Amidyl Radicals Controlled by Vinylic Halogen Substitution. *Org. Lett.* **2006**, *8*, 2647–2650. [CrossRef]
64. Wang, F.; Zhang, X.; He, Y.; Fan, X. Selective Synthesis of Pyrrolidin-2-Ones and 3-Iodopyrroles via The Ring Contraction and Deformylative Functionalization of Piperidine Derivatives. *Org. Biomol. Chem.* **2019**, *17*, 156–164. [CrossRef]

65. Pandeeti, O.; Bijigiri, S.K.; Panda, P.K. One-Pot Synthesis of Benzotripyrrole Derivatives from 1H-Pyrroles. *New J. Chem.* **2019**, *43*, 18437–18841. [CrossRef]
66. Zeng, X.; Liu, S.; Yang, Y.; Yang, Y.; Hammond, G.B.; Xu, B. Regio- and Stereoselective Synthesis of 1,2-Dihaloalkenes Using In-Situ-Generated ICl, IBr, BrCl, I_2, and Br_2. *Cell Press Chem.* **2020**, *6*, 1018–1031. [CrossRef]
67. Betz, R.; Klüfers, P. 1-Bromomethyl-2-Iodobenzene. *Acta Crystallogr. Sect. E: Struct. Rep. Online* **2007**, *63*, o4753. [CrossRef]
68. Mamane, V.; Peluso, P.; Aubert, E.; Cossu, S.; Pale, P. Chiral Hexahalogenated 4,4′-Bipyridines. *J. Org. Chem.* **2016**, *81*, 4576–4587. [CrossRef] [PubMed]
69. Lehnherr, D.; Alzola, J.M.; Lobkovsky, E.B.; Dichtel, W.R. Regioselective Synthesis of Polyheterohalogenated Naphthalenes via the Benzannulation of Haloalkynes. *Chem. Eur. J.* **2015**, *21*, 18122–18127. [CrossRef] [PubMed]
70. Barát, V.; Csókás, D.; Bates, R.W. Synthesis of (−)-Cytisine Using a 6-Endo Aza-Michael Addition. *J. Org. Chem.* **2018**, *83*, 9088–9095. [CrossRef] [PubMed]
71. Tian, J.; Luo, F.; Zhang, Q.; Liang, Y.; Li, D.; Zhan, Y.; Kong, L.; Wang, Z.-X.; Peng, B. Asymmetric Iodonio-[3,3]-Sigmatropic Rearrangement to Access Chiral α-Aryl Carbonyl Compounds. *J. Am. Chem. Soc.* **2020**, *142*, 6884–6890. [CrossRef]
72. Shi, Q.; Zhang, S.; Zhang, J.; Oswald, V.F.; Amassian, A.; Marder, S.R.; Blakey, S.B. KO^{t}Bu-Initiated Aryl C–H Iodination: A Powerful Tool for the Synthesis of High Electron Affinity Compounds. *J. Am. Chem. Soc.* **2016**, *138*, 3946–3949. [CrossRef] [PubMed]
73. Zhang, S.; Wang, W.; Li, C.; Liu, P.; Xu, W.; Tang, L.; Wang, J.; Zhao, G. Facile Synthesis of Enantiomerically Pure 1-(5-Bromo-2-Chlorophenyl)-1-(4-Ethoxyphenyl)ethane. *Chem. Res. Chin. Univ.* **2014**, *30*, 250–256. [CrossRef]
74. Sun, K.; Zhang, S.; Liu, Z.; Lv, Y. Eco-Friendly C–I and C–O Bond Formation of Simple Alkenes: Direct Access to β-Iodo Oxyamines. *Chem. Sel.* **2018**, *3*, 5766–5768. [CrossRef]
75. Gelbrich, T.; Threlfall, T.L.; Hursthouse, M.B. XPac Dissimilarity Parameters as Quantitative Descriptors of Isostructurality: The Case of Fourteen 4,5′-Substituted Benzenesulfonamido-2-Pyridines Obtained by Substituent Interchange Involving CF_3/I/Br/Cl/F/Me/H. *CrystEngComm* **2012**, *14*, 5454–5464. [CrossRef]
76. Mukherjee, A.; Desiraju, G.R. Halogen Bonds in Some Dihalogenated Phenols: Applications to Crystal Engineering. *IUCrJ* **2014**, *1*, 49–60. [CrossRef]
77. Caracelli, I.; Haiduc, I.; Zukerman-Schpector, J.; Tiekink, E.R.T. M···π(arene) Interactions for M = Gallium, Indium and Thallium: Influence upon Supramolecular Self-Assembly and Prevalence in Some Proteins. *Coord. Chem. Rev.* **2014**, *283*, 50–63. [CrossRef]
78. Balmohammadi, Y.; Khavasi, H.R.; Naghavi, S.S. Existence of Untypical Halogen-Involving Interactions in Crystal Packings: A Statistical and First-Principles Study. *CrystEngComm* **2020**, *22*, 2756–2765. [CrossRef]
79. Politzer, P.; Murray, J.S. The Use and Misuse of van der Waals Radii. *Struct. Chem.* **2021**, *32*, 623–629. [CrossRef]
80. Sakurai, T.; Sundaralingam, M.; Jeffrey, G.A. A Nuclear Quadrupole Resonance and X-Ray Study of Crystal Structure of 2,5-Dichloroaniline. *Acta Crystallogr.* **1963**, *16*, 354–363. [CrossRef]
81. Desiraju, G.R.; Parthasarathy, R. The Nature of Halogen···Halogen Interactions - Are Short Halogen Contacts due to Specific Attractive Forces or due to Close Packing of Nonspherical Atoms. *J. Am. Chem. Soc.* **1989**, *111*, 8725–8726. [CrossRef]
82. Rheingold, A.L. Private Communication to the Cambridge Structural Database. *Refcode COMJUM* **2019**. [CrossRef]
83. Liu, R.; Wu, W.Y.; Li, Y.H.; Deng, S.P.; Zhu, H.J. 2-Bromo-5-Iodo-1, 3-Dimethylbenzene. *Acta Crystallogr. Sect. E Struct. Rep. Online* **2008**, *64*, o280. [CrossRef]
84. Bhar, A.; Aune, J.P.; Benali-Cherif, N.; Benmenni, L.; Giorgi, M. Three Polychloromononitrobenzenes: $C_6H_3Cl_2NO_2$, $C_6H_2Cl_3NO_2$ and $C_6HCl_4NO_2$. *Acta Crystallogr. Sect. C Cryst. Struct. Commun.* **1995**, *51*, 256–260. [CrossRef]
85. Näther, C.; Jess, I.; Kuś, P.; Jones, P.G. Dimorphism of 1,4-Dibromo-2,5-bis(bromomethyl)benzene: Crystallographic and Physicochemical Investigations. *CrystEngComm* **2016**, *18*, 3142–3149. [CrossRef]
86. Kersten, K.; Kaur, R.; Matzger, A. Survey and Analysis of Crystal Polymorphism in Organic Structures. *IUCrJ* **2018**, *5*, 124–129. [CrossRef] [PubMed]
87. Sacchi, P.; Lusi, M.; Cruz-Cabeza, A.J.; Nauha, E.; Bernstein, J. Same or Different – That Is the Question: Identification of Crystal Forms from Crystal Structure Data. *CrystEngComm* **2020**, *22*, 7170–7185. [CrossRef]
88. Guo, M.L.; Zhang, L. 2,4-Dibromo-6-(4-bromophenyliminomethyl)phenol. *Acta Crystallogr. Sect. E Struct. Rep. Online* **2007**, *63*, o4558. [CrossRef]
89. Ji, H.; Ma, H.P.; Yang, Y.A.; Zhu, H.L. 2-[(4-BromPhenylimino)methyl]-4,6-Diiodophenol. *Acta Crystallogr. Sect. E Struct. Rep. Online* **2012**, *68*, o788. [CrossRef]
90. Zhang, X.L.; Guo, Y.N. Crystal Structure of 2-Bromo-4-Chloro-6-[(4-Bromophenylimino)methyl]phenol, $C_{13}H_8Br_2ClNO$. *Z. Kristallogr. New Cryst. Struct.* **2011**, *226*, 521–522. [CrossRef]
91. Zhang, X.L. Crystal Structure of 2-Bromo-4-Chloro-6-[(4-chlorophenylimino)methyl]phenol, $C_{13}H_8BrCl_2NO$. *Z. Kristallogr. New Cryst. Struct.* **2011**, *226*, 567–568. [CrossRef]
92. Puthilibai, G.; Vasudhevan, S.; Rajagopal, G. 2-Bromo-4-Chloro-6-(4-fluorophenyliminomethyl)phenol. *Acta Crystallogr. Sect. E Struct. Rep. Online* **2008**, *64*, o1333. [CrossRef] [PubMed]
93. Yang, Z.M.; Zhu, H.; Zhu, H.L. Crystal Structure of 2[(4-Fluorophenylimino)methyl]-4,6-Diiodophenol, $C_{13}H_8FI_2NO$. *Z. Kristallogr. New Cryst. Struct.* **2012**, *227*, 447–448. [CrossRef]
94. Dunitz, J.D.; Taylor, R. Organic Fluorine Hardly Ever Accepts Hydrogen Bonds. *Chem. Eur. J.* **1997**, *3*, 89–98. [CrossRef]

95. Tiekink, E.R.T.; Zukerman-Schpector, J. A Structural Survey of Meta$\cdots\pi$ Heteroaromatic Supramolecular Synthons for Metal =Tellurium, Tin, and Gold. *CrystEngComm* **2009**, *11*, 2701–2711. [CrossRef]
96. Allen, F.H.; Motherwell, W.D.S.; Raithby, P.R.; Shields, G.P.; Taylor, R. Systematic Analysis of the Probabilities of Formation of Bimolecular Hydrogen-Bonded Ring Motifs in Organic Crystal Structures. *New J. Chem.* **1999**, *23*, 25–34. [CrossRef]